Journal of Next-Generation Research 5.0 (JNGR 5.0)
E-ISSN: 3075-2868 Website: www.jngr5.com Email: editor@jngr5.com

Comparison of Meshless and Finite Element Methods for Elastic–Plastic Assessment of HIPPS Pressure Vessels

Giulio Malinverno
FIMAC S.p.A., Via Piemonte 19, 20030 Senago (MI), Italy
Email: g.malinverno@fimac.aero

Abstract
This article compares the meshless method and the classical finite element method in the case of elastic-plastic analysis of pressure vessels. The finite element method has proven to be a robust approach over the years and has been continuously developed for both static and dynamic analyses, as well as linear and nonlinear applications. However, the use of the finite element method presents some intrinsic critical issues, such as the generation of the calculation grid or mesh and dependence, leading to the introduction of methods that do not require the explicit generation of a calculation grid, or meshless methods. The purpose of this paper is to review the performance of a meshless resolution compared with the traditional mesh-based approach, in the case of the verification of industrial HIPPS valves, focusing on the precision and quality of the results obtained as well as the operating cost, assessing the method's operational advantages at an industrial level.

Keywords: Meshless methods; Elastic–plastic analysis; Pressure vessels; HIPPS; ASME BPVC.

1. Introduction

The structural analysis of valves used as final elements in protection systems is a requirement expressed by different standards whose purpose is to ensure the introduction of reliable and safe systems on the market.

Alongside the traditional analytical methods based on the Lamé, Mariotte and Barlow formulas, the advent of electronic calculators and the spread of suites[1] based on the finite element method has made the verification of pressure vessels through numerical simulation traditional. The transition to numerical methods is justified not only by the possibility of obtaining results that are more responsive to reality but also by the possibility of considering more load configurations at more reasonable costs if compared to traditional experimental tests [1].

[1] The term suite is preferable, in the opinion of the writer, to the term solver, because, although the actual solution is calculated by the solver, the engineer who is designing or verifying a structure must first prepare the mathematical model to submit to the solver and then analyze the results obtained from the resolution. In both phases, the use of dedicated and reliable programs has the same importance as the solver, as the computer science principle known as GIGO (garbage in, garbage out) applies.

The finite element method has proven to be a robust method over the years and has been continuously developed for both static and dynamic analyses, linear and non-linear, in both the field of solid and fluid mechanics[2][1]. However, the use of the finite element method presents some intrinsic critical issues, such as the generation of the calculation grid (mesh) and the dependence of the results on mesh characteristics, leading to mesh-dependent outcomes, particularly when dealing with large deformations or discontinuities [2–4].

It follows that the engineer who is preparing to carry out a finite element analysis must pay due attention to the generation of the calculation grid and, subsequently to the generation of the results, their critical analysis to determine whether pathologies related to the mesh may have influenced the results. The most direct consequence is the time required for the correct generation of the calculation grid, especially in the presence of particular geometries and with large variations in shapes and sections.

One of the solutions proposed to overcome these problems is the elimination of the issue at its root, namely the removal of the calculation mesh in the numerical solution of partial differential equations, as stated by Liu [2].

The introduction of numerical methods that do not require the explicit generation of a calculation grid, or meshless methods, allows us to overcome the problems highlighted in the previous paragraph, since meshless methods (also known as meshfree) do not require the connection between the nodes of the simulation domain via a grid (i.e. the information is conveyed via the elements), but are based on the interaction of each node with all its neighbors[3].

Meshless methods were initially introduced where large deformations or flows of matter were required, such as in computational fluid dynamics or in simulations of plastic materials, as the use of a traditional mesh introduced errors and results that did not correspond to reality [2,5–7].

A further field of application of meshless methods is fracture mechanics, both in the field of classical mechanics [4,8,9], biomechanics [10], and geotechnical analyses [11,12].

Although they do not introduce a conceptual advantage in the field of classical structural checks (small deformations and validity of the continuum hypothesis), meshless methods have begun to spread mainly due to the greater efficiency of preparation of the mathematical model, especially in the case of complex geometries, which therefore require a considerable expenditure of resources in terms of man-hours. The purpose of this paper is to compare the meshless or meshfree numerical resolution method with the traditional mesh-based finite element method, and to verify its applicability in the verification of pressure vessels, such as valves used as final elements (valves) of a HIPPS protection system, described in the next paragraph.

---

[2] Traditionally, in computational fluid dynamics (CFD) analyses, finite difference or finite volume methods are used, which are “relatives” of the finite element method. Furthermore, in recent years, in parallel with the introduction of “multiphysics” simulations, the finite element method has been directly applied in solving fluid dynamic problems.

[3] With the added advantage that the “neighbors” can change over time / course of the simulation, while in the case of FEM, the node / element correlation is fixed and immutable

In particular, the verification will focus on the following points:

- comparison of the precision and quality of the results obtained with a meshless method,
- operating cost of the meshless method.

In fact, it will be verified not only that the meshless method is adequate to obtain the results with an acceptable precision but also that its application is operationally advantageous at an industrial level, i.e. that it requires a lower overall time than that necessary for a traditional finite element simulation.

2. Engineering Background

The purpose of this paper is to compare the elastic-plastic analysis of the pressure components that constitute the final element of a HIPPS system. High Integrity Pressure Protection Systems (HIPPS) are safety instrumented systems (SIS), assemblies dedicated to the protection of an industrial plant, such as a petrochemical plant or an offshore platform, or part of these plants, intervening in the event of overpressure recorded in the plant's supply line.

A HIPPS system is normally made up of three fundamental elements:

- initial elements, i.e. the measuring instruments whose task is to "start" the action,
- the control logic which, once the measuring signals have been collected, interprets them and determines the intervention of the system,
- the final elements, consisting of the valve assembly plus the relative actuator.

Usually, in order to guarantee the required level of reliability, there are several final elements, logically arranged in parallel. The physical arrangement instead depends on the implemented safety function, i.e. the safety operation can be to close or open the valves. Respectively, the valves will be physically arranged in series and in parallel.

Since the valve that constitutes the final element can be classified not only as a component of a safety instrumented system but also as a pressure accessory, its design and verification fall under stringent regulations and codes, such as the PED directive (2014/68/EU) [13] and the IEC 61508/61511 standards. The latter specifications require that the system and its components be verified for systematic failures (i.e. have a verified and robust design), as well as for random failures. Therefore, it follows that the manufacturer of a valve for a HIPPS system must perform countless tests and checks before placing his device on the market, checks that are normally performed through numerical analysis and simulations.

Valves are mechanisms or machines that control the flow of a fluid and its pressure through functions like shut-off, throttling of the intensity of the flow and/or the downstream pressure, or act as pressure relief. There are many models and types of valves that satisfy one or more of the functions identified above, with a multitude of types and designs that adapt to a wide variety of industrial applications. Regardless of type, all valves can be considered as a pressure vessel from a structural point of view. The main pressure containing parts that composed a valve can be summarized as follows:

- Body,
- Closure or bonnet
- Gland flange or Trunnion.

In this paper, the analyses were executed on a valve body, but the methodologies here described can be applied to each component as well as their assembly.

The body, also referred to as shell, is the main pressure element of the valve and transmits / supports the loads deriving from the pipes (being the valves connected to the pipe through the body threaded, bolted or welded joints), as well as acting as a container for the elements regulating the flow.

3. Applied Methodology

Valves are classified at the regulatory level as pressure accessories, both for European legislation, i.e. the PED directive [13], and for American industrial standards, such as API 6A [14], 6D [15], 6DSS [16], and 17D [17] which require the application of the design codes for pressure equipment (ASME BPVC sec. VIII [18]) for valve design.

In particular, considering the wall dimensions and geometries of a valve, it is industrial practice that the verification is carried out through the application of the design-by-analysis methodology defined by part 5 of the ASME BPVC sec. VIII div. 2 [18], which provides for the following checks:

- Verification of protection against static loads, in particular:
  - Verification of protection against plastic collapse.
  - Verification of protection against local collapse.
- Verification of protection against instability.
- Verification of protection against cyclic loads, divided into:
  - Verification against ratcheting,
  - Verification against fatigue.

The traditional linear assessment is based on the comparison of the stress derived from the loads applied to the component and the maximum allowable stress, derived from the characteristics of the material (yield stress or ultimate load, appropriately reduced by a safety factor)

The stresses to be compared with the admissible ones are obtained through the simplified formulation (Mariotte - Barlow) of the Lamé formulas, in the case of analytical verification, or through numerical resolution with the finite element method, and categorized according to whether they contribute to the equilibrium or have a self-equilibrated local effect. The fundamental assumption of this methodology is that of the perfectly elastic behavior of the material, the small deformations and the consequent validity of the principle of superposition of effects. It follows that the overall number of analyses can be reduced by considering the individual acting loads and then exploiting the superposition of effects.

This approach has the undoubted advantages of expressing the results in terms of:

- quantities easily interpretable such as the stresses

or, given the linearity of the approach,

- safety margins.

Given the result of the analyses for a set of loads, the designer can then understand the magnitude of the stress in the case of a combination of loads and also understand how much the loads can be increased (i.e., how much the thickness can be decreased) without invalidating the design verification.

However, due to the complex geometry and thickness of valve's pressure containing part, the above-mentioned hypothesis could be no more applicable, and the traditional assessment could especially around structural discontinuities, may produce non-conservative results and is not recommended by the applicable code [18].

The code, thus, indicates in the load and resistance factor design method (with an elastic-plastic formulation of the structural materials) the preferred assessment method with complex or thick geometries. The assessment consists in the application of properly factored loads coupled with an elastic-plastic formulation of materials. For each load case combination (global collapse, local failure, etc.) a proper assessment criterion is provided.

In this paper, since we were interested in comparing the results obtainable using a meshless methodology in the elastic–plastic field, verification analyses were conducted to assess protection against global collapse, local failure, and fatigue due to cyclic loading.

3.1 Assessment Against Global Collapse

Under the action of the factored load, the structure under consideration may not be able to reach an equilibrium configuration and support the loads or transmit them to the foundations. The verification of protection against global collapse consists in verifying that the structure can assume an equilibrium configuration such as to support the loads. This verification has been designed with numerical resolutions in mind.

In fact, both traditional finite element analysis and meshless analysis consist in solving the algebraic equations on the displacements obtained by discretizing the differential equilibrium equations. As such, these resolutions are not in closed form, but approximate solutions obtained through numerical iterations. The convergence of the method is monitored by the solver itself and has a very precise intrinsic physical meaning: once convergence has been obtained, the structure has reached a stable configuration consistent with the applied loads and constraints.

Since the numerical solver is not able to handle rigid motions, in the case of rigid motions, the solver will not be able to find a congruent solution and therefore reach convergence: rigid motions can be generated by two distinct conditions. The first is when the mathematical model has not been properly created and the constraints applied in such a way as not to prevent rigid motions. This condition is easily verified by applying modest loads and verifying that convergence has been achieved. The other mechanism by which rigid motions can develop is when the forces applied to the structure are greater than its load-bearing capacity, as there will be indefinite deformations and a rigid motion of the structure or parts of it.

Consequently, in a properly constrained model, the rigid motion of the structure (or part of it) is an unequivocal sign that structural collapse has occurred. That is, the convergence of the solution implies the achievement of an equilibrium configuration congruent with the loads and constraints and therefore satisfaction of the global criterion.

3.2 Assessment Against Local Failure

Protection against local failures, i.e. the creation of unstable plastic hinges in localized areas of the structure, occurs with the evaluation of the plastic deformations at each point of the structure and verify that it does not exceed an admissible value.

For a generic load condition, the following must be obtained:

$$\varepsilon_{peq} + \varepsilon_{cf} < \varepsilon_L \quad (1)$$

Where:

- ε_{peq} is the equivalent plastic deformation evaluated through numerical simulation,
- ε_{cf} is the residual deformation resulting from stamping or forging processes,
- ε_{peq} is the maximum triaxial deformation for the material subjected to the load considered.

The maximum triaxial strain is evaluated as

$$\varepsilon_L \doteq \varepsilon_{LU} \exp\left[-\left(\frac{\alpha_{sl}}{1+m_2}\right)\cdot\left(\frac{\sigma_1+\sigma_2+\sigma_3}{3\sigma_e}-\frac{1}{3}\right)\right] \quad (2)$$

Where:

- ε_{LU} is the maximum uniaxial strain of the material,
- α_{sl} and m_2 are parameters related to the material typology and defined by the code (18),
- σ_i are the principal stresses given by the load condition considered,
- $\sigma_e \doteq \frac{1}{\sqrt{2}}\cdot[(\sigma_1-\sigma_2)^2+(\sigma_2-\sigma_3)^2+(\sigma_3-\sigma_1)^2]^{0.5}$ is the von Mises equivalent stress.

It should also be noted that, although at first glance the verification of protection against local failures may seem to be a classic ASD approach, as the actual deformations are compared with the allowable ones, in reality the approach is actually non-linear as the value of the allowable triaxial strain is determined by the stress tensor currently applied – it follows that by varying the loads and their combination, this value undergoes variations that are not necessarily linear.

In case of multiple load conditions, a concept similar to the accumulated damage for fatigue can be introduced. Defining the damage for the ith load condition as (strain limit damage):

$$D_{\varepsilon,i} \doteq \frac{\varepsilon_{L,i}}{\varepsilon_{peq,i}+\varepsilon_{cf}} \quad (3)$$

In order for the protection against local failure to be verified, it must be that:

$$D_\varepsilon \doteq \sum D_{\varepsilon,i} \leq 1 \quad (4)$$

3.3 Assessment Against Cyclic Loads

The procedure for fatigue verification is based on the analysis of the load history using for example an algorithm such as the rainflow method or the min-max method (in order to obtain an ordered sequence of loads representing the cycles) and on the stresses and deformations obtained through a numerical simulation and applying appropriate calculation methods such as the Twice Yield Method developed by Kalnins [19,20].

The rainflow method is defined by the ASTM E1409 standard and is recommended by the code to determine the times that represent the unique load cycles where the variation in time of the loads, stresses and deformations can be identified by a single parameter. The cycles counted with the Rainflow method correspond to closed stress-strain hysteresis loops, with each loop representing a cycle.

The min-max method is recommended where there are non-proportional loads and stresses/deformations. The cycle counting is performed by first building the largest cycle, using the highest peak and the lowest valley, then further cycles are built taking peaks and valleys in descending order, until all the peaks are exhausted.

The Twice Yield Method is based on an elastic-plastic structural analysis performed in a single loading phase, considering a stabilized stress-strain curve, in which a loading interval represents a cycle of the loading history. Stress and deformation are the direct result of this analysis. The advantage of this method is that it is possible to use a monotonic analysis without any loading-unloading cycle. In other words, it is possible to think of performing a single multi-step analysis, in which the load is applied in a monotonically increasing manner and each step represents a cycle of the loading history. For each component and for each load cycle (therefore, using the twice yield method for each load step), the ranges of stresses ($\Delta S_{p,k}$) and plastic deformations ($\Delta \varepsilon_{peq,k}$) are evaluated. Having applied the twice yield method, the range of stresses and deformations correspond to the stresses and deformations of the single load step. We then proceed to evaluate the effective range of deformations for the kth cycle (step):

$$\Delta \varepsilon_{eff,k} = \frac{\Delta S_{P,K}}{E_{ya,k}} + \Delta \varepsilon_{peq,k} \tag{5}$$

And subsequently the equivalent alternating stress for the cycle considered:

$$S_{alt,k} = \frac{E_{ya,k} \cdot \Delta \varepsilon_{eff,k}}{2} \tag{6}$$

From the S-N curves provided by the code, we then calculate the maximum number of cycles allowed N_k for the stress found and therefore the accumulated damage:

$$D_{f,k} = \frac{n_k}{N_k} \tag{7}$$

Having indicated with n_k the number of cycles expected for the load condition considered. In order for the fatigue test to be satisfied, the sum of all accumulated damage must not exceed unity:

$$\sum_{k=1}^{M} D_{f,k} \leq 1.0 \tag{8}$$

3.4 Linear Elastic Assessment

In addition to the elastic-plastic analysis, the same models have been simulated under nominal loads conditions (i.e., no factored loads) with a simple linear elastic material formulation, in order to retrieve stress, strain, and the execution time also for this type of simulation.

3.5 Comparison Methodology

The results will be compared with each other taking as a reference the stress and deformation values obtained through the finite element method the dense calculation grid.

Since the program used to evaluate the meshless method has fixed outputs, we will not proceed to evaluate the local criterion according to ASME, but we will focus only on the values of

- Stress

- Equivalent elastic deformation (total)
- Plastic deformation

The simulation execution times will also be evaluated.
In order to have a more balanced comparison, machines with equivalent capacity and computing power will be used, in particular using the same number of processors for the resolution.

4. Resolution Methods and Solvers

4.1 The Finite Element Method and Solvers

CAE simulation tools, usually based on finite element method, are extremely important because they allow them to validate the performance or optimize the design of a product before the product itself is physically created.
The finite element method is based on the variational or discrete formulation of the problem to be solved and on the discretization of the integration domain in quantized calculation cells, i.e. the finite elements: the finite element method involves the transformation of a continuous problem into a discrete algebraic problem, with the obvious advantage of decreasing the resolution complexity of the problem [21].
This is achieved by spatially discretizing the problem: the real domain is divided into enough elementary subdomains (elements), characterized by being connected to each other via points (nodes). The continuity of the domain is then lacking since the various elements are only connected pointwise. Within the single element, the solution that is desired is expressed through a series development. Note that the discretization is at a spatial level, since the development is done through continuous functions although different from element to element.
The fundamental parameters of the solution are then referred to the interconnection nodes between the elements, so that the information can be transmitted from element to element.
Furthermore, the elements into which the domain is divided do not generally have arbitrary shapes but it is preferable to use standard normalized elements (obviously different from time to time depending on the physical problems involved): in this way the properties of the elementary domain, expressed through the N functions, are calculated upstream on normalized elements and subsequently referred to the real domain of the problem with appropriate coordinate transformations.
Based on this development, even the applied loads, or more generally the boundary conditions of the problem, are concentrated in the nodes, through the same methodology adopted for the mechanical characteristics.
The advantages of such an approach are various and can be summarized as:

- a simpler solution approach (of an algebraic type),
- a lower computational cost (compared with the strong resolution of the PDEs),
- the precision of the solution can be modified by increasing or decreasing the spatial discretization of the domain.

On the other hand, the method involves significant disadvantages:

- the solution obtained is not “exact” because deduced from:
    - a weak (variational) form and not strong approach,

- a numerical calculation on discretized domains,

- the solution strongly depends on the modeling adopted and therefore the same problem can be addressed in different ways with different results (for example, because a load that is actually distributed has been concentrated).

The typical workflow of a finite element resolution is shown in the following ***Figure 1***.

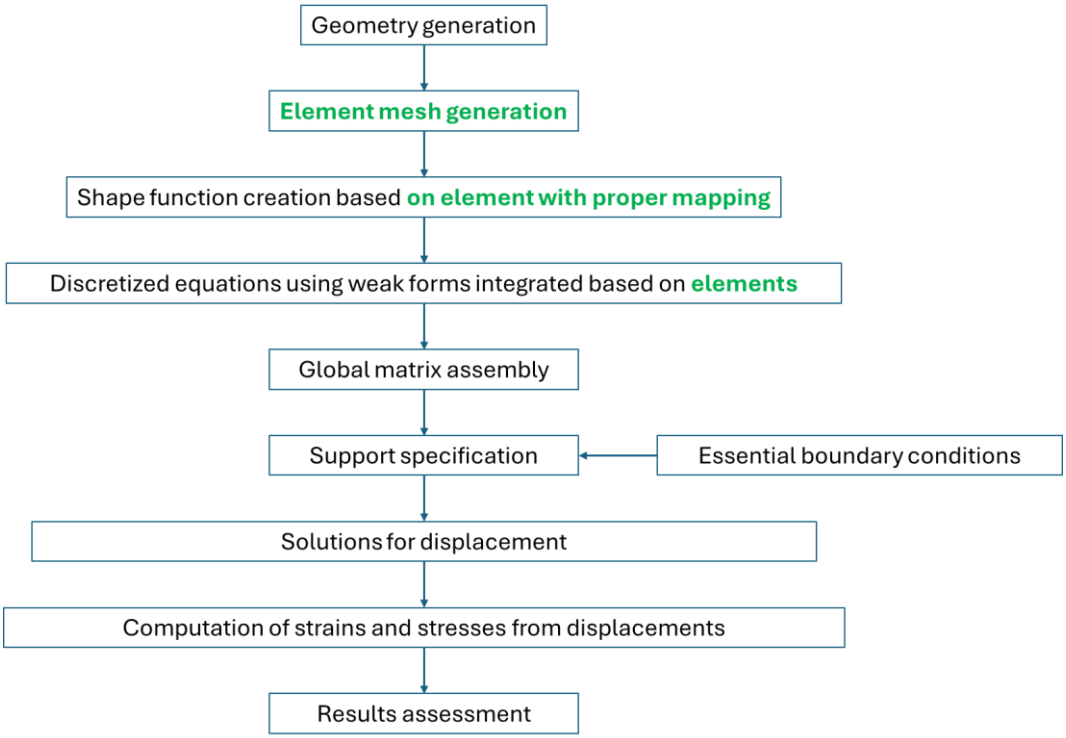

Figure 1. Finite Elements Traditional Workflow

4.1.1 ANSYS Workbench and SimScale (Code ASTER)

To retrieve the finite element results, three models/solvers have been considered:

- An engineering acceptable (coarse) mesh, with a majority of prismatic elements, solved with ANSYS mechanical solver,
- A refined mesh, with a majority of prismatic elements, solved with ANSYS mechanical solver,
- An engineering acceptable (coarse) mesh, with a majority of tetrahedral elements, solved with Code ASTER (SIMSCALE implementation) online solver.

The rationale of this selection consists in the comparison of already known tools, with the meshless solver, and an online tool. For the latter, the basic mesh configuration was chosen, with a view to comparing the operational methodology in the design phase, where it is preferable to obtain a result in a short time and the detailed checks (with more refined meshes) are left to a later phase.

ANSYS Workbench is a suite of programs dedicated to the numerical simulation of physical problems, from structural calculations to thermo-fluid dynamics. It is composed of several tools ranging from a solid modeler for cleaning operations and possibly the creation of geometries, a graphical interface for the creation of the calculation grid and the application of boundary conditions

and loads as well as the analysis of the results downstream of the analysis, as well as obviously the actual finite element solver. The latter is recognized at industrial level and its validation is not normally required, also having an extensive bibliography attesting to the validity of the resolutions. For comparison, a commercial implementation (on cloud) of the open-source finite element solver Code Aster was also used (via the SIMSCALE platform).

4.2 The Meshless Method and Meshless Solver

As highlighted by Liu [2], the weak link in the traditional approach based on the finite element method is the intrinsic need to create the computational grid (mesh) that is both accurate and efficient.

The computational grid generation process can fail miserably if performed directly on the original geometry of the studied object as conceived by the designer, in the case of complex objects or with numerous details, for example due to fillets or chamfers of negligible size compared to the other dimensions of the part. Alternatively, the grid can be generated but with an excessive number of elements that make its analysis highly inefficient in an industrial context, especially during the product development phase.

Furthermore, the grid generation could result in elements that are too distorted that compromise the analysis results, for example by causing stress concentrations beyond the material limits.

In the case of products consisting of multiple parts, moreover, incompatible grids on adjacent parts make resolution difficult and can give rise, as above, to unusable results.

It follows that the simplification of the geometric model of the piece studied requires experience and foresight on the part of the modeler, having first to interpret the physical phenomena and introduce into the model the simplifications necessary to obtain on the one hand a model consistent with the reality to be studied and on the other a model that can be easily analyzed and that gives usable results.

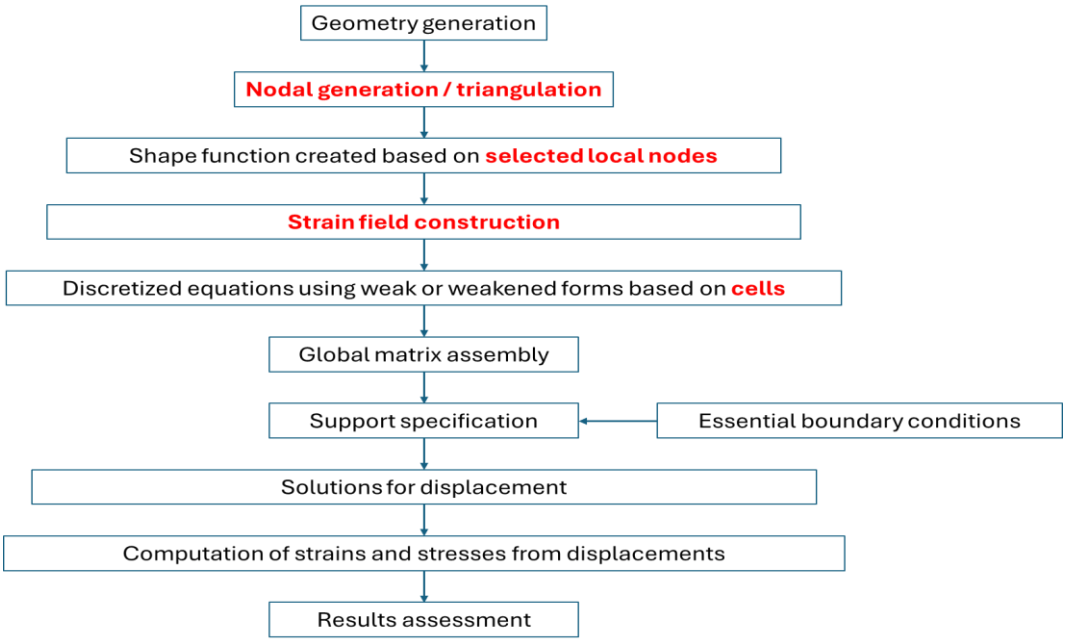

Figure 2. Meshless Method Workflow

Meshfree or meshless methods (whose workflow is shown in Figure 2) aim to overcome the aforementioned problems by addressing them at their root [2,3], namely by eliminating the need to define a calculation grid *a priori*. In these approaches, the domain of interest is no longer represented by a grid of nodes and elements (i.e., elements interconnected through nodes), but is discretized solely by a set of arbitrarily distributed nodes. The solution is then based on the interaction of each node with its surrounding nodes, with the shape functions defined only over the domain (or a portion of it) and the nodes contained therein.

Thus, meshless methods and the traditional finite element method are both based on the weak formulation of the differential problem. Both are based on the three key points highlighted in the previous paragraphs:

- the construction of the shape functions,
- the integration on the domain,
- the weak form used to create the discrete algebraic system to be solved numerically.

The field variable (displacement, stress or strain) at each point within the domain of study is approximated or interpolated using the nodes within a given "support domain" within the chosen node.

$$u(x) = \sum_{i \in S_n} \phi_i(x) \cdot u_i \tag{9}$$

Where:

- S_n is the set of local nodes included in the support domain, in a local (bounded) domain of the considered point,
- u_i is the field variable at the ith nodal point,
- $\phi_i(x)$ is the nodal shape function, the shape function of the i-th node created using all the support nodes contained in the support domain.

Please note that the interpolation defined by the previous equation is generally performed for all components of all field variables in the same support domain: for example, if one is interested in the displacement field, the same shape function is used for all three displacement components. However, there may be situations where one can use different shape functions – for example, to calculate deflection and torsion in structural simulations, in order to avoid shear-locking and membrane-locking phenomena. The "support domain" of a generic point x determines the number of nodes that will be used to approximate the function at the point x. This support domain can be "weighted" using functions that vanish on the boundary of the domain.

For the construction of the shape functions for a generic point x_0, the nodes that contribute to the definition of this shape function are those whose domain of influence covers point x.

The use of distributed nodes not only allows to overcome the problems seen in the previous paragraph but also offers further advantages – for example the possibility of increasing their number in the stress concentration zones without having to worry about their relationships with pre-existing nodes, or, increasing the propagation zone of a crack to evaluate its stress and propagation.

Since it is not necessary to generate a quality calculation grid, and since the nodes can be positioned in an automated way, the times traditionally required by an engineer / analyst for the generation of the mesh can be avoided, an obvious saving for companies.
In meshless methods, shape functions are based on a point or cell of the domain, using a small number of local modes, selected in the vicinity of the cell or reference point – thus the shape function depends on the local position in the domain and the construction of shape functions in meshless analyses occurs during the analysis itself.

- Integration in meshfree methods is based on the background cells / nodes, directly or indirectly with various approaches, among which we can mention:
- Using directly the cells created for the domain (similarly to FEM) (Element Free Galërkin method);
- Using smooth domains based on nodes created from the original cells (Node-based smoothed Point Interpolation Method, NS-PIM);
- Using smooth domains based on edges created from the original cells (Edge-based Smoothed Point Interpolation Method, ES-PIM);
- Using triangular sub-cells created by further subdividing the original cells, (Cell-based Smoothed Point Interpolation Method, ES-PIM or Constructed Point Interpolation Method, SC-PIM).

4.2.1 External Approximation Method

The ALTAIR SIMSOLID® solver is based on the theory of external finite element approximations , [22,23] which are a generalization of the finite element method, where:

- Arbitrary geometric shapes can be used as “finite elements” – note that here the term “finite element” is used to designate an arbitrarily shaped subdomain of the Ω domain, so the definition of a finite element is no longer limited to canonical shape functions or other shapes obtained from a canonical shape by mapping. One could then consider the entire domain as a finite element, i.e. for assemblies, a part of an assembly could be a “finite element” in FEM terminology
- The basis functions that approximate the field of interest can be of an arbitrary class and are independent of the shape of the volume – the functions no longer need to be polynomial, and the only requirement is that they are sufficiently “smooth” inside the element.

Since the continuity of shape functions in the classical finite element method is only guaranteed at the local level, the success of the finite element method has shown that the continuity and continuity of derivatives requirements can / must be satisfied only to a certain extent. The extension of this approach of relaxing the continuity requirements has led to the concept of “external approximations”, where the term external must be understood as external to the space of finite strain energy functions (Sobolev’s space).
Altair SIMSOLID is a program for solving structural problems (static and dynamic) based on meshless methods. ALTAIR's response to the market demand for streamlining numerical simulations was precisely to implement a meshless method as a replacement for the traditional FE method, rather than through improvements to the user interface.

All the complexities traditionally associated with the generation of the calculation grid (from geometry simplification to grid quality control) are obviously not present in SIMSOLID since the real geometry of the object or system to be analyzed is processed directly. Assemblies can have parts with different thicknesses and dimensions (large / small or thick / thin).
The time required to set up the simulation model is consequently significantly shorter and, furthermore, the reduction of the required process phases also leads to a reduction in the possibility of error by the user.
To further refine the solution, an adaptive refinement process has been introduced by default during the solution process.
The workflow in ALTAIR SIMSOLID can be summarized as follows:

- Import the geometry from CAD – as mentioned, it is not necessary to "clean up" the geometry.
- In the case of assemblies, define the connections between the various parts – the connections are normally already recognized by the program as "glued" or "mutual sliding", they must be modified if necessary, according to the need.
- Define the analysis parameters – such as the type of analysis (linear or nonlinear structural statics, thermal, modal, etc.).
- Define the convergence criterion – in the static structural field it is possible to choose between:
  - convergence on stiffness,
  - convergence on stresses,
  - a custom defined convergence criterion.
- Apply boundary conditions and loads.
- Solve the problem, with adaptive methods.
- Post-process / analyze the results.

5. Problem Modelling

5.1 Pressure Vessel Description

The element that is most characterized as a pressure vessel is the valve body and given the limitations of the simulation programs, only this component has been analyzed according to the checks discussed in the previous paragraphs. Due to the geometry selected, exploiting symmetry properties, only a quarte of model has been considered Figure 2.

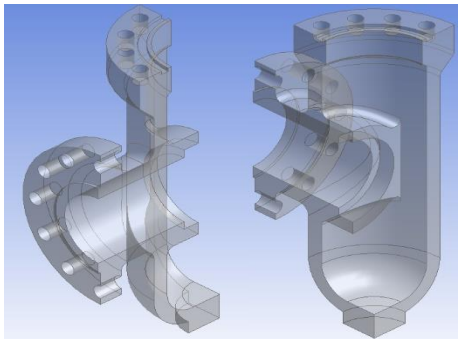

Figure 2. Valve Body, Quarter Model

The perfect simulation would be the one that completely reconstructs the physical object and all the boundary conditions of the problem considered, in other words, the reproduction of the environment in which the object of study is inserted. It goes without saying that such a mathematical model would be unusable, as it would necessarily be too complex and expensive.
The purposes of modeling can be summarized as:

- reproducing physical reality in an advantageous way, i.e. the reproduction of physical reality occurs by introducing simplifications aimed at reducing the computational cost of simulations, so that the simulations themselves can be carried out in reasonable times and with physically coherent results,
- closing the mathematical problem and allowing numerical resolution, i.e. modeling has the task of closing the mathematical problem, applying appropriate boundary conditions.

Since the simplifications introduced must not alter the physics of the problem, it is therefore essential to first understand which effects we are interested in and which components, details and conditions greatly influence these effects.
In this case, being interested in the study of the body as a pressure vessel, the effects of the other components of the valve, such as closure, or of the environment in which the valve is located, cannot be neglected, but also not directly modeled.
The simplification of the real model in this case was therefore reduced to the extraction of the body from the valve and the introduction, as constraints and loads, of the effects due to the environment and the other components of the valve.
In detail, the pressure forces due to the pipes were introduced directly on the body as forces applied to the end flanges, while the effect of the closure and the related linkage was simulated through the translation constraint on the vertical. In fact, since the pressure vessel, in its entirety, is a self-balanced body, the effect of the pressure on the closure and the effect of the linkage are equal and opposite to the effects of the pressure on the body itself. In fact, this is precisely the definition of the constraints on the displacements in physical terms.
As for the constraint on the translation to the other directions, it is obtained by exploiting the symmetry of the geometry and the applied loads, which allows the use of a quarter of the model.
The use of symmetries also allows not only to reduce the computational cost but also to apply natural boundary conditions that do not introduce constraints on the movements of the structure.

The two surfaces parallel to the symmetry planes were therefore constrained to the normal displacements of the surfaces themselves, while the vertical translation was suppressed (Figure 4).

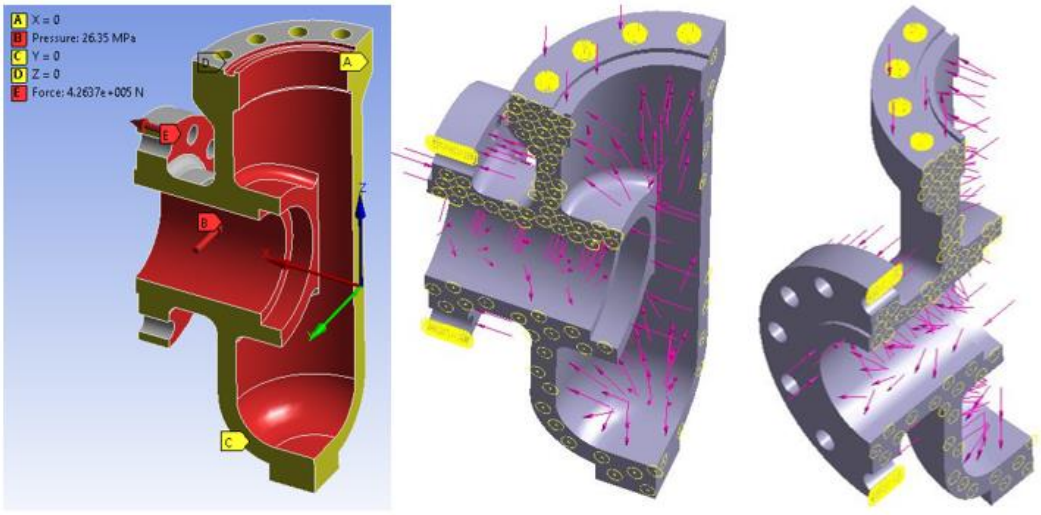

Figure 4. Boundary Conditions and Loads Applied, ANSYS Model (Left) and Altair (Right)

5.2 Mesh Description

In the case of finite element simulations, it was necessary, as known, to prepare the discretization of the calculation domain in elements.

As a good engineering practice in order to improve the numerical results with the same number of elements and nodes (especially in this case, where using the non-commercial (Student) Version of ANSYS, the total number of elements is set to 32,000), the calculation grid was created by applying the following options:

- Activation of the elastic-plastic options ("plasticity options – shape checking: nonlinear mechanical analysis");
- Having forced the solver to generate prismatic elements ("hexahedral dominant"), where impossible (i.e. where elements too distorted would have been generated), the selection fell on tetrahedral elements.

20-node second-order hexahedral elements (SOLID 186) and 10-node tetrahedral elements (SOLDI 187) were used [24] (see also Figure 5).

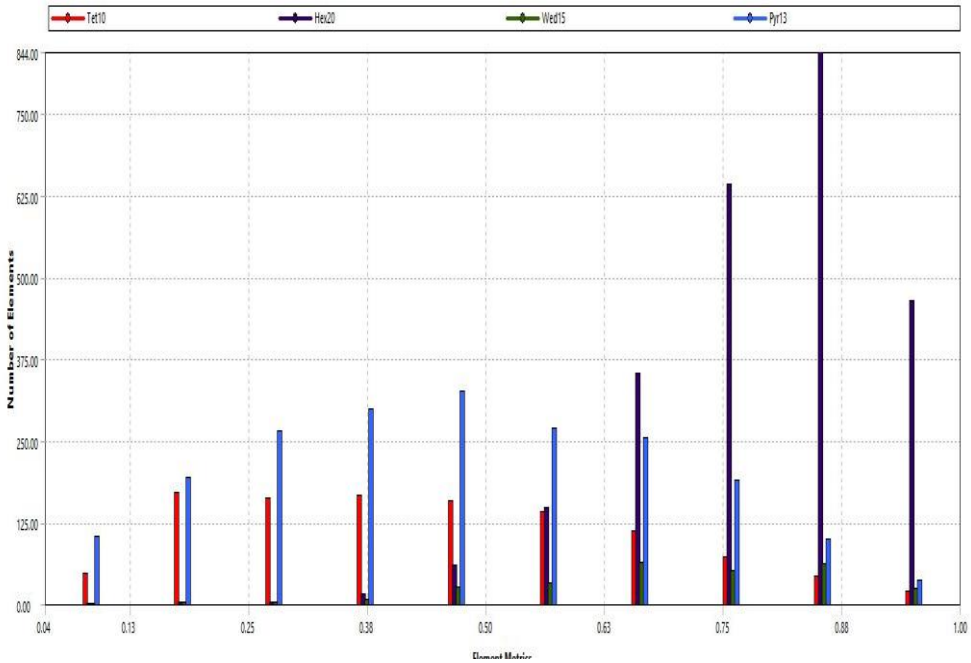

Figure 5. Mesh Metrics, ANSYS Coarse Mesh

Due to software limitations on the maximum number of elements for the simulation, a maximum element size of 20 mm was defined – lower values would have increased the number of elements beyond the permitted limit. The calculation grid was thus rather sparse in some areas, particularly in the pipeline and in the seat impost, where only two elements are present. The choice of adopting second-order elements helps to overcome this shortcoming and obtain reasonable results of engineering interest.

To verify the goodness of the finite element model, a more refined model (~ 193'000 nodes) was developed using the commercial license of ANSYS (mesh metrics shown in Figure 6).

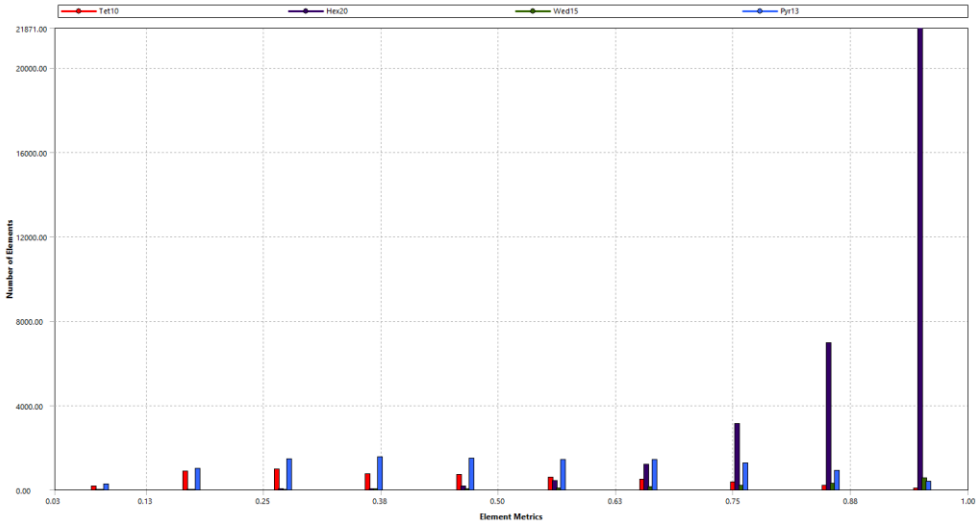

Figure 6. Mesh Metrics, ANSYS Refined Mesh

Journal of Next-Generation Research 5.0 (JNGR 5.0)
E-ISSN: 3075-2868 Website: www.jngr5.com Email: editor@jngr5.com

Additionally, as said, in previous par. 0, a third solver has been considered. For this solver, the basic mesh configuration was chosen, with a majority of tetrahedral elements.
A visual comparison of the meshed model is displayed in the following Figure 3.

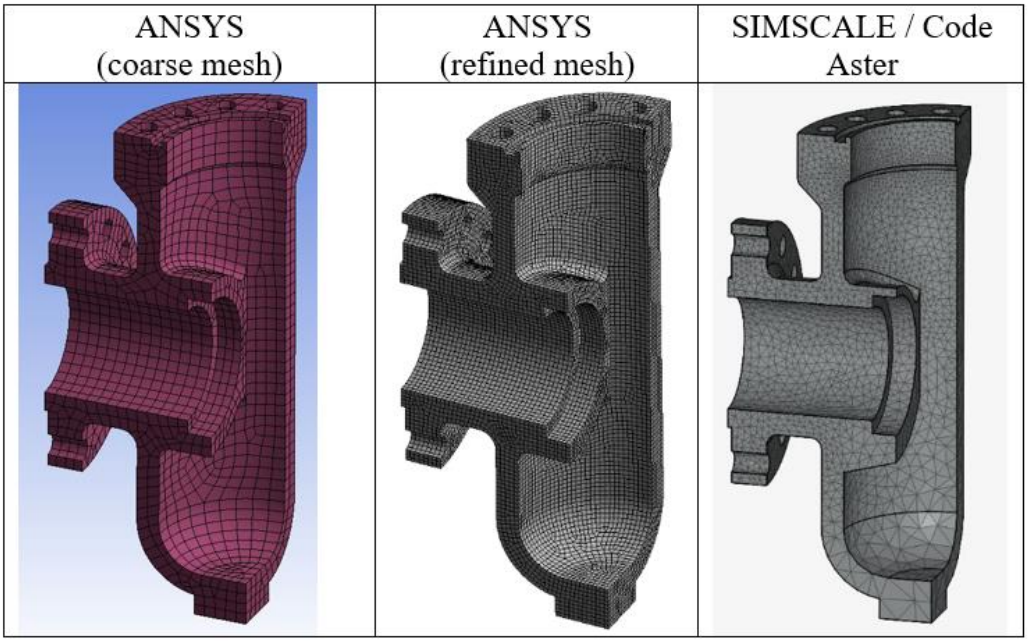

Figure 3. Finite Element Models' Mesh

5.3 Material Formulation

5.3.1 Elastic Plastic Formulation for Global and Local Collapse

The verification methodology described by ASME BPVC sec. VIII div. 2 part 5 [18] for static elastic-plastic analyses (protection against plastic collapse, local verification and instability) requires that the material is described by an appropriate stress-strain curve that includes the plastic part. The 3D appendix of the code describes how to obtain the elastic-plastic curve of a ductile metallic material given some characteristics such as yield, unit load at break, specific elongation, Poisson's modulus:

$$\varepsilon_t = \frac{\sigma_t}{E_y} + \gamma_1 + \gamma_2 \tag{10}$$

With:

$$\mathrm{m}_2 = 0.75 \cdot (1 - R) \qquad m_1 \doteq \frac{\ln(R) + (\varepsilon_p - \varepsilon_{ys})}{\ln\left(\frac{\ln(1+\varepsilon_p)}{\ln(1+\varepsilon_{ys})}\right)} \qquad \varepsilon_\mathrm{p} = 2.0 \cdot 10^{-5}$$

$$\gamma_1 \doteq \frac{\varepsilon_1}{2}(1 - \tanh(H)) \qquad A_1 \doteq \frac{\sigma_{ys}(1+\varepsilon_{ys})}{(\ln(1+\varepsilon_{ys}))^{m_1}} \qquad \varepsilon_1 \doteq \left(\frac{\sigma_t}{A_1}\right)^{\frac{1}{m_1}} \tag{11}$$

$$\gamma_2 \doteq \frac{\varepsilon_2}{2}(1 + \tanh(H)) \qquad A_2 \doteq \frac{\sigma_{uts}\exp(m_2)}{m_2^{m_2}} \qquad \varepsilon_2 \doteq \left(\frac{\sigma_t}{A_2}\right)^{\frac{1}{m_2}}$$

$$\sigma_{uts,t} \doteq \sigma_{uts} \exp(m_2) \qquad H \doteq \frac{2\left(\sigma_t - \left(\sigma_{ys} + K\left(\sigma_{uts} - \sigma_{ys}\right)\right)\right)}{K\left(\sigma_{uts} - \sigma_{ys}\right)} \qquad \varepsilon_{ys} \doteq 0.002$$

$$K \doteq 1.5R^{1.5} - 0.5R^{2.5} - R^{3.5} \qquad R \doteq \frac{\sigma_{ys}}{\sigma_{uts}}$$

Please note that parameters m_2 and ε_p are defined by the code for several materials. The values here indicated refer to stainless steel and nickel-based alloys.

Please also note that in the numerical simulation, as indicated in article 5.2.4.4 of the code, the simulation must use real stress and not engineering ones, that is, the curve must be extended up to the true ultimate stress, defined by the value:

$$\sigma_{uts,t} \doteq \sigma_{uts} \exp(m_2) \tag{12}$$

It can be noted that the elastic-plastic formulation requires more parameters for the construction of the curve, unlike the classic methods based on the elastic formulation of the material, where only two parameters are strictly necessary, the Poisson's modulus and the Young's modulus (or another equivalent parameter, e.g. the shear modulus).

5.3.2 Elastic-Plastic Formulation for Fatigue Analysis

In a similar way, in the case of the elastic-plastic verification of the protection against fatigue phenomena, the calculation code provides for the use of a Ramberg-Osgood type curve in paragraph 3-D.4 of [18], formulated as follows:

$$\varepsilon_{ta} = \frac{\sigma_a}{E_y} + \left(\frac{\sigma_a}{K_{CSS}}\right)^{\frac{1}{n_{CSS}}} \tag{13}$$

This relationship links the amplitude of the deformations to the amplitude of the stresses and, to take into account the hardening and the hysteresis loops, can be rewritten as:

$$\varepsilon_{tr} = \frac{\sigma_r}{E_y} + 2 \cdot \left(\frac{\sigma_r}{2 \cdot K_{CSS}}\right)^{\frac{1}{n_{CSS}}} \tag{14}$$

Please note that the coefficients K_{CSS} and n_{CSS} are provided by the code only for some generic families of materials, and not for specific material. In the case of exotic or non-tabulated materials, such as duplex steels, it is necessary to refer to the specific literature to obtain the coefficients K_{CSS} and n_{CSS} necessary for the analysis. Theoretically, the parameters of interest are obtained with expensive and long experimental fatigue test campaigns - however, there are theoretical formulations that are close to the experimental results and based on the properties of the materials obtainable through classical tensile tests, as described in the works of Marohnic et alt. , [25,26], Lopez and Fatemi [27], or Zhang et alt. [28].

In particular, the Lopez and Fatemi formulation, [25,27] is easy to implement and has excellent experimental correlation, and it is described as follows:

$$K_{CSS} = \begin{cases} 1.16 \cdot \sigma_{uts} + 593 \; per \; \dfrac{\sigma_{uts}}{\sigma_{ys}} > 1.2 \\ 3.0 \cdot 10^{-4} \cdot \sigma_{uts}^2 + 0.23 \cdot \sigma_{uts} + 619 \; per \; \dfrac{\sigma_{uts}}{\sigma_{ys}} \leq 1.2 \end{cases} \quad (15)$$

and

$$n_{CSS} = -033 \cdot \frac{\sigma_{ys}}{\sigma_{uts}} + 0.4 \quad (16)$$

Once the equivalent alternating stress values have been obtained, the number of admissible cycles can be obtained using a classic Wöhler SN curve depending on the material considered. The code provides the curves for the most commonly used families of materials and there is normally no need to search for other data.

Furthermore, the curves are calibrated according to the basic philosophy of the code, as indicated by Kalnins , [19,20] that is, the danger index considered here is the crack nucleation. Using curves from other sources could lead to a methodological error as the danger indices would be different and the safety margins required by the code would be distorted.

6. Results

6.1 Structural Analysis Results Comparison

Since all simulations have reached convergence, it is possible to state that each solver is able to solve the elastic-plastic assessment against the global collapse, i.e. the pressure vessel is able to sustain the factored loads with no general collapse.

The distribution of stress and strains is similar in all four simulation methodologies, both for the case of the verification against local failures and the fatigue verification. The meshless method correctly identifies the same critical regions as the finite element method, as shown in Figure 8.

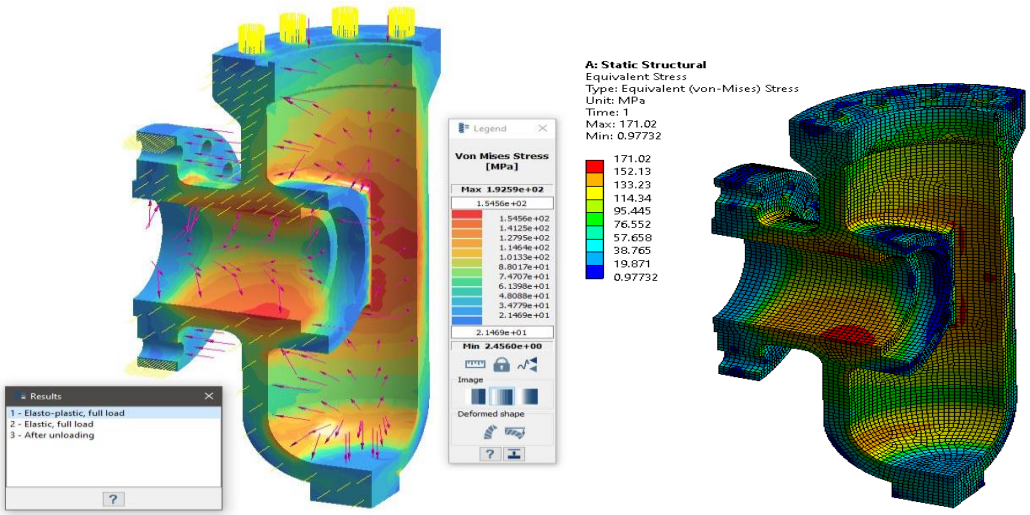

Figure 8. Stress Distribution, Meshless Method (Stress Convergence Approach, Left) and Finite Element Method (Right)

However, considering the specific values, which must be used for ASME checks, the results seen in the previous paragraphs demonstrate without any doubt how the settings made at the level of the mathematical model, both in the case of the classic finite element method and in the more recent meshless approach, heavily influence the results. This is evident by making a value-by-value comparison for the various configurations analyzed, as shown in Table 1

Table 1. Assessment of local Failure Results

	Stress (MPa)	*Strain Total (mm/mm·10^{-3})*	*Strain elastic (mm/mm·10^{-3})*	*Strain Plastic (mm/mm·10^{-3})*
ANSYS (coarse mesh)	158.76	1.506	0.873	0.633
ANSYS (refined mesh)	171.02	1.547	0.899	0.648
SIMSCALE	168.90	1.809	0.919	0.890
SIMSOLID (Stress convergence)	192.59	2.440	1.210	1.230
SIMSOLID (Strain convergence)	173.48	1.662	1.02	0.642

As for the classic finite element method, using second order elements and hexahedrons, the use of a fairly sparse calculation grid provides stress differences of up to 10%, while there is greater precision on the deformations. This behavior can be seen in both the assessments (i.e. local failures and assessment against fatigue), a sign that the material formulation does not influence the calculation (see Tables 2 and 3).

Table 2. Assessment of Cyclic Load Results

	Stress (MPa)	*Strain Total (mm/mm·10^{-3})*	*Strain elastic (mm/mm·10^{-3})*	*Strain Plastic (mm/mm·10^{-3})*
ANSYS (coarse mesh)	154.36	0.863	0.846	0.0165
ANSYS (refined mesh)	142.55	0.860	0.817	0.0428
SIMSCALE	152.6	0.876	0.811	0.0645
SIMSOLID (Stress convergence)	144.12	0.798	0.614	0.184
SIMSOLID (Strain convergence)	143.1	0.732	0.590	0.142

Table 3. Linear Elastic Results

	Stress (MPa)	*Strain elastic (mm/mm·10^{-3})*
ANSYS (coarse mesh)	140.20	0.701
ANSYS (refined mesh)	147.20	0.736
SIMSCALE	197.80	0.989
SIMSOLID (Stress convergence)	195.53	0.978
SIMSOLID (Strain convergence)	145.96	0.730

In the case of analyses conducted with the meshless method, as well as in the case of tetrahedral meshes, assuming that the value recovered from the finite element analyses with the fine mesh is the "real" values, it can be observed that:

- the values calculated by privileging convergence on stiffness are normally more aligned than those obtained with convergence on stresses,
- the total and plastic deformations obtained with convergence on stresses are significantly higher,
- the total deformations, in both cases, are very high.

Since no analytical solutions or experimental data are available, to compare the results it is possible to consider the results obtained with the refined mesh solved with ANSYS® as the "good" solution, and, thus, evaluate how far the other solvers (and mesh) are. The percentage differences between the results are reported in Tables 4 and 5.

Considering the values obtained using the nominal pressure and the linear material formulation, smaller differences and comparable calculation times are observed (see Table 6).

Table 4. Percentage Difference Between Solvers, Local Failure Analysis

	ΔStress (%)	*ΔStrain Total (%)*	*ΔStrain elastic (%)*	*ΔStrain Plastic (%)*
ANSYS (coarse mesh)	-7.169	-2.650	-2.892	-2.315
SIMSCALE	-1.240	16.936	2.225	37.346
SIMSOLID (Stress convergence)	12.613	57.725	34.594	89.815
SIMSOLID (Strain convergence)	1.438	7.434	13.459	-0.926

Table 5. Percentage Difference Between Solvers, Cyclic Load Analysis

	ΔStress (%)	*ΔStrain Total (%)*	*ΔStrain elastic (%)*	*ΔStrain Plastic (%)*
ANSYS (coarse mesh)	8.285	0.349	3.550	-61.449
SIMSCALE	7.050	1.86	-0.734	50.701
SIMSOLID (Stress convergence)	1.101	-7.209	-24.847	329.907
SIMSOLID (Strain convergence)	0.386	-14.884	-27.785	231.776

Table 6. Percentage Difference Between Solvers, Linear Elastic Results

	ΔStress (%)
ANSYS (coarse mesh)	-4.755
SIMSCALE	34.375
SIMSOLID (Stress convergence)	32.833
SIMSOLID (Strain convergence)	-0.842

6.2 Execution Time Comparison

In terms of timing, the use of the meshless method has effectively eliminated the time needed for designing and generating the calculation grid, including the "cleaning" times of the geometric model. However, it is noted that the calculation times for elastic-plastic solutions, especially in the case of verification against plastic collapse and local failures, are greatly superior to the time required by the finite element solver, having in fact, for the first solution, execution times in the order of tens of minutes, to be compared with the few minutes of an FE analysis with the refined grid.

The main cause is the use of material nonlinearities that have introduced additional iterations for convergence – in fact, in the fatigue analysis, which presents a very weak plasticization (if not zero, in the vicinity of the numerical error), the calculation times are aligned with those of the finite element method with a sparse grid (a few seconds). In fact, if we consider the values relating to the calculation with the nominal pressure and the linear formulation of the material, we have smaller differences and comparable calculation times between the selected solvers.

The calculation times for the simulation in ALTAIR SIMSOLID refer to the resolution of the various simulations, conducted individually. Please note that ALTAIR SIMSOLID allows you to solve the system by favoring the convergence of stress rather than that on stiffness. With the same initial conditions, by running the simulation again by changing only the target (for example by first setting the convergence on the stresses and then that on the stiffness), the second simulation is much faster, starting from the results of the first.

Please note that Tables 7 and 8 report the solver execution time (and the corresponding percentage differences); therefore, the time spent on mesh generation and model setup is not included.

Table 7. Solver Execution Time

	Execution time – global and local collapse (s)	*Execution time – cyclic loads (s)*	*Execution time – linear elastic (s)*
ANSYS (coarse mesh)	38	12	10
ANSYS (refined mesh)	179	69	60
SIMSCALE	180	600	50
SIMSOLID (Stress convergence)	1931	8	79
SIMSOLID (Strain convergence)	11	8	7

Table 8. Percentage Difference Between Solvers, Execution Time

	ΔExecution time – global and local collapse (s)	*ΔExecution time – cyclic loads (s)*	*ΔExecution time – cyclic loads (s)*
ANSYS (coarse mesh)	-78.78	-82.61	-83.33
SIMSCALE	+0.559	+769.56	-16.67
SIMSOLID (Stress convergence)	+978.77	-88.41	+31.67
SIMSOLID (Strain convergence)	-93.85	-88.40	-88.33

7. Conclusions

This article summarized the analyses conducted to compare traditional FE method and the meshless approach in the assessment of a pressure containing part as per ASME BPVC sec. VIII div.2. The analyses demonstrated that the meshless method has excellent potential in terms of ease of use of the software and setting of the physical problem, freeing the analyst from the task of preparing a refined calculation grid.

However, the values obtained from the meshless analysis in the nonlinear context are quite different from those obtained with the classic finite element methods and this contributes to undermining confidence in these methods. On the other hand, the differences found are comparable to those obtainable with the finite element method in the case of different mesh types and this reconfirms how the preparation of the calculation grid is critical.

Furthermore, the calculation times required are, at least as far as the model examined is concerned, markedly higher than those required by the finite element simulation, and if we consider the overall times, given by the sum of the times required for modeling and simulation, there is no obvious advantage when final verification analyses need to be performed on the product.
In light of the fact that the results obtained in the linear field differ less, and that for the linear analysis the efforts to validate the project are sufficient, as well as the execution times are significantly reduced, the meshless methodology seen can be introduced as a support tool for designers in the initial design phase, where a rapid estimate of the efforts and the possibility of comparing multiple engineering solutions in a short time are recurring needs.

Author Contributions Statement
G.M. conceived of the presented idea. G.M. developed the theoretical formalism and the algorithm, performed the numerical simulations and wrote the main manuscript.

Funding Statement
All authors declare that they have no conflicts of interest.
No funding was received.

References
1. Cesari F. *Il Metodo degli Elementi Finiti Applicato al Moto dei Fluidi*. Bologna: Pitagora Editrice; 1986.
2. Liu GR. *Meshfree Methods*. Boca Raton (FL): CRC Press; 2009.
3. Belytschko T, Liu WK, Moran B, Elkhodary KI. *Nonlinear Finite Elements for Continua and Structures*. New York: John Wiley & Sons; 2014.
4. Auricchio F, Guarnaschelli F. *Alternativa al Metodo degli Elementi Finiti nella Meccanica della Frattura: gli X-FEM*. Master's Thesis. Milan: Politecnico di Milano; 2010.
5. Ghozzi Y, Labergere C, Villon P. Numerical Simulation Based on Meshless Formulation: Application to 2D Solid Mechanics. In: *Proceedings of the ASME 2012 International Mechanical Engineering Congress and Exposition*. New York: American Society of Mechanical Engineers; 2012. p. 439–447.
6. Idelsohn SR, Oñate E, Calvo N, Del Pin F. The Meshless Finite Element Method. Int J Numer Methods Eng. 2003;58(6):893–912.
7. Zovatto L, Nicolini M. The Meshless Approach for the Cell Method: A New Way for the Numerical Solution of Discrete Conservation Laws. Int J Comput Eng Sci. 2003;4(4):869–880.
8. Liu J, Yan B, Jiang N. Computational Method for Crack-Opening Area of Nuclear Pressure Pipe with Circumferential Through-Wall Crack. In: *Proceedings of the 18th International Conference on Nuclear Engineering*. New York: ASME; 2010. p. 499–503.
9. Liu SJ. Meshless Simulation of Fracture in Thin-Walled Pipe Structures. In: *Proceedings of the ASME Pressure Vessels and Piping Conference*. New York: ASME; 2009. p. 273–280.

10. Pani M, Marson I, Tonti E. *Sviluppo, Valutazione e Applicazione di Metodi Numerici Alternativi al Metodo degli Elementi Finiti in Problemi di Biomeccanica Ortopedica*. PhD Thesis. Trieste: Università degli Studi di Trieste; 2009.
11. Ma J, Summers JD, Joseph PF. Meshless Integral Method for Analysis of Elastoplastic Geotechnical Materials. In: *Proceedings of the ASME IDETC/CIE Conference*. New York: ASME; 2010. p. 153–163.
12. Bortolami S, Cola S, Ceccato F. *Propagazione di Flussi Granulari e Impatto sulle Strutture Analizzati Mediante Approccio MPB*. Master's Thesis. Padova: Università degli Studi di Padova; 2016.
13. European Parliament, Council of the European Union. *Directive 2014/68/EU on Pressure Equipment*. Official Journal of the European Union; 2014.
14. American Petroleum Institute. *API Specification 6A: Specification for Wellhead and Christmas Tree Equipment*. Washington (DC): API; 2010.
15. American Petroleum Institute. *API Specification 6D: Specification for Pipeline and Piping Valves*. Washington (DC): API; 2014.
16. American Petroleum Institute. *API Specification 6DSS: Specification for Subsea Pipeline Valves*. Washington (DC): API; 2009.
17. American Petroleum Institute. *API Recommended Practice 17D: Design and Operation of Subsea Production Systems – Subsea Wellhead and Tree Equipment*. Washington (DC): API; 2011.
18. American Society of Mechanical Engineers. *ASME Boiler and Pressure Vessel Code, Section VIII, Division 2*. New York: ASME; 2015.
19. Kalnins A. Fatigue Analysis in Pressure Vessel Design by Local Strain Approach: Methods and Software Requirements. J Press Vessel Technol. 2006;128(1):2–7.
20. Kalnins A. Twice-Yield Method for Assessment of Fatigue Caused by Fast Thermal Transient According to ASME BPVC Section VIII, Division 2. In: *Proceedings of the ASME Pressure Vessels and Piping Conference*. New York: ASME; 2008. p. 63–71.
21. Malinverno G. *Aeroelasticità Applicata*. Italy: Lulù; 2007.
22. Apanovitch V. *The Method of External Finite Element Approximations*. Independently Published; 2021.
23. Apanovitch V. Using Altair SimSolid Technology Overview. Altair. https://altair.com/docs/default-source/resource-library/altair_whitepaper_simsolid-technology-overview_10_30_2020.pdf. Accessed July 3, 2025.
24. ANSYS Inc. *ANSYS Mechanical APDL Documentation: Element Library, Version 17.1*. Canonsburg (PA): ANSYS Inc; 2016.
25. Marohnić T, Basan R, Franulović M. Evaluation of the Possibility of Estimating Cyclic Stress-Strain Parameters and Curves from Monotonic Properties of Steels. Procedia Eng. 2015;101:277–284.
26. Marohnić T, Basan R, Franulović M. Evaluation of Methods for Estimation of Cyclic Stress-Strain Parameters from Monotonic Properties of Steels. Metals (Basel). 2017;7(1):17.

27. Lopez Z, Fatemi A. A Method of Predicting Cyclic Stress–Strain Curve from Tensile Properties for Steels. Mater Sci Eng A. 2012;556:540–550.
28. Zhang Z, Qiao Y, Sun Q, Li C, Li J. Theoretical Estimation of the Cyclic Strength Coefficient and the Cyclic Strain-Hardening Exponent for Metallic Materials: Preliminary Study. J Mater Eng Perform. 2009;18(3):245–254.